

# Crystal Structure of a Homogeneous IgG-Fc Glycoform with the N-Glycan Designed to Maximize the Antibody Dependent Cellular Cytotoxicity

Chia-Lin Chen,<sup>†,‡,§,Ⓛ</sup> Jen-Chi Hsu,<sup>†</sup> Chin-Wei Lin,<sup>†,‡,Ⓛ</sup> Chia-Hung Wang,<sup>⊥</sup> Ming-Hung Tsai,<sup>⊥</sup> Chung-Yi Wu,<sup>†,‡</sup> Chi-Huey Wong,<sup>\*,†,‡,§,Ⓛ,Ⓛ</sup> and Che Ma<sup>\*,†,‡</sup>

<sup>†</sup>Genomics Research Center, Academia Sinica, Taipei, Taiwan

<sup>‡</sup>Chemical Biology and Molecular Biophysics program, Taiwan International Graduate Program, Academia Sinica, Taipei, Taiwan

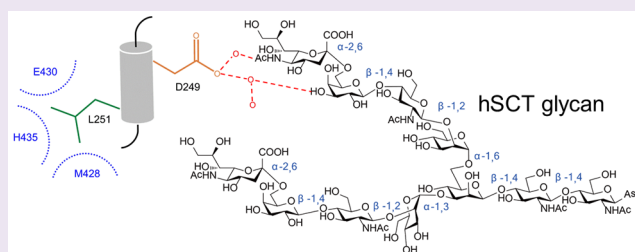
<sup>§</sup>Institute of Biochemical Sciences, National Taiwan University, Taipei, Taiwan

<sup>Ⓛ</sup>Department of Chemistry, National Taiwan University, Taipei, Taiwan

<sup>⊥</sup>CHO Pharma Inc., Taipei, Taiwan

## S Supporting Information

**ABSTRACT:** N-glycosylation on IgG modulates Fc conformation and effector functions. An IgG-Fc contains a human sialo-complex type (hSCT) glycan of biantennary structure with two  $\alpha$ 2,6-sialylations and without core-fucosylation is an optimized glycoform developed to enhance the antibody dependent cellular cytotoxicity (ADCC). hSCT modification not only enhances the binding affinity to Fc receptors in the presence of antigen but also in some cases provides gain-of-function effector activity. We used enzymatic glyco-engineering to prepare an IgG-Fc with homogeneous hSCT attached to each C<sub>H</sub>2 domain and solved its crystal structure. A compact form and an open form were observed in an asymmetric unit in the crystal. In the compact structure, the double glycan latches from the two hSCT chains stabilize the C<sub>H</sub>2 domains in a closed conformation. In the open structure, the terminal sialic acid (N-acetylneuraminic acid or NeuNAc) residue interacts through water-mediated hydrogen bonds with the D249–L251 helix, to modulate the pivot region of the C<sub>H</sub>2–C<sub>H</sub>3 interface. The double glycan latches and the sialic acid modulation may be mutually exclusive. This is the first crystal structure of glyco-engineered Fc with enhanced effector activities. This work provides insights into the relationship between the structural stability and effector functions affected by hSCT modification and the development of better antibodies for therapeutic applications.



Antibody immunoglobulin G (IgG) plays a pivotal role in host defense through its ability to recognize and eradicate foreign pathogens. IgGs are large biomolecules with a mass of approximately 150 kDa, built from two heavy chains and two light chains. From functional and structural viewpoints, IgG can be divided into two Fab domains and one Fc domain, responsible for antigen-recognition and effector functions, respectively. Recombinant monoclonal IgGs are an emerging class of protein drugs with applications in diagnosis and therapeutic treatments. They have been introduced for treating cancers (e.g., Rituxan and Herceptin), infectious diseases, or autoimmune disorders.<sup>1</sup> Despite the presence of divergent Fab sequences for targeting different antigens in various diseases, recent studies indicate that the Fc region also displays a considerable diversity for antibody functions. For example, IgG which binds to the tumor surface marker would be further recognized by the Fc receptors or C1q, which then activates the antibody dependent cellular cytotoxicity (ADCC) or complement dependent cytotoxicity (CDC), respectively, to eliminate tumor cells.<sup>2,3</sup> In addition, the Fc domain bound to the neonatal Fc receptor determines the half-life and recycling of

antibodies, while which cellular receptor can bind to sialylated IgG for immune inhibitory effect remains to be answered.<sup>4–7</sup>

Like other extracellular glycoproteins, IgGs also undergo glycosylation in the ER and Golgi networks in the cells. The C<sub>H</sub>2 domain of each heavy chain contains one N-glycosylation site at the N297 position. The core structure of Fc N-glycan is a hepta-saccharide composed of four N-acetylglucosamines (GlcNAcs) and three mannoses: two GlcNAcs and one mannose on the stem and one mannose and one GlcNAc on each of the two arms. This can be further extended with galactose, sialic acid, core fucose, and bisecting GlcNAc. Although the Fc domain is highly conserved in the protein sequence, the diverse N-glycosylation has been shown to modulate its conformations and effector functions. For example, deglycosylated IgG shows a closed structure with a very narrow space between the C<sub>H</sub>2 domains, thus reducing

Received: February 15, 2017

Accepted: March 20, 2017

Published: March 20, 2017

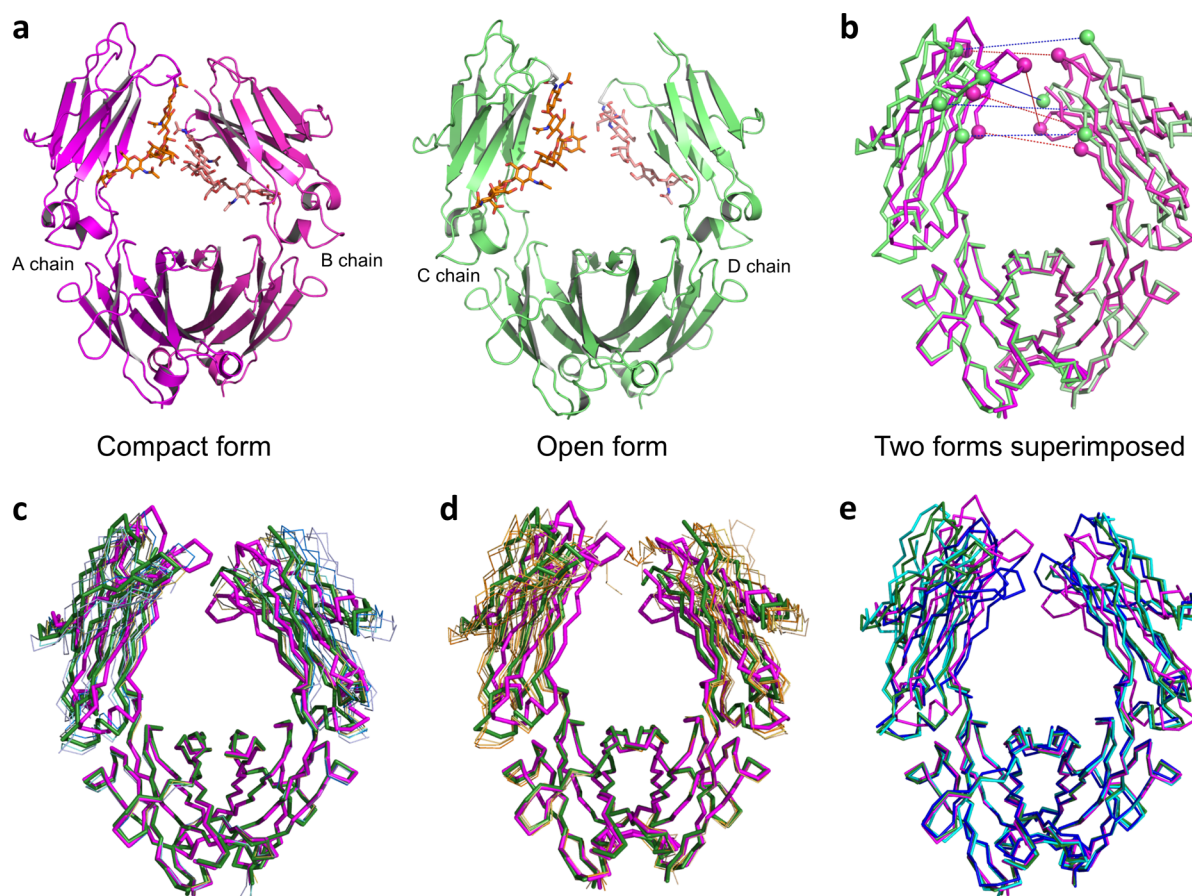


**Figure 1.** Crystal structure of Fc<sub>hSCT</sub>. (a) Two forms of Fc<sub>hSCT</sub> structure. Structures are drawn in cartoon representation, while N-glycosylation sites and N-glycans are shown as sticks. Compact form (A, B chains) and open form (C, D chains) of Fc<sub>hSCT</sub> are colored in magenta and green, respectively. (b) Superimposition of two dimers in an a.s.u. of Fc<sub>hSCT</sub> crystal. The distances between paired Cα atoms (F241, N297, R301, and P329) are shown as red and blue lines in A–B chains and C–D chains, respectively. (c) Alignment of Fc<sub>hSCT</sub> with Fc containing different glycoforms or mutations. (PDB entries: 3DO3 (gray), 4KU1 (marine), 2WAH (blue), 3DNK (cyan), and 5D4Q (yellow)). (d) Alignment of Fc<sub>hSCT</sub> with Fc in complex with FcγRIIIA. (PDB entries: 3AY4 (light orange), 3SGJ (orange), 3SGK (bright orange), 3WN5 (wheat), 5D6D (yellow)). (e) Alignment of Fc<sub>hSCT</sub> with two forms of di-sFc (PDB entry: 4Q6Y): Open form of di-sFc (cyan) and closed form of di-sFc (blue). All structures are aligned by superimposing the C<sub>H3</sub> domains.

receptor binding and deactivating effector function.<sup>8,9</sup> Core-fucosylation and bisecting N-acetylglucosamylation occur in a mutually exclusive manner.<sup>2,10</sup> Core-fucosylation of IgG-Fc affects binding to Fc γRIIIA, with nonfucosylated antibodies exhibiting higher ADCC activity.<sup>11,12</sup> Galactose addition is reported to increase anti-inflammatory activity, while a low level of galactosylation on IgGs is a common feature in various diseases, such as rheumatoid arthritis and primary osteoarthritis.<sup>13</sup> Terminal sialic acid extension of IgG also shows anti-inflammatory properties, although the detailed mechanism and the interaction with receptors are not yet clearly defined.<sup>5–7,14</sup>

N-glycosylation of IgG has a critical impact on its biological functions; thus a key emphasis in the pharmaceutical industry for the production of monoclonal antibodies involves the control and optimization of N-glycan profiles.<sup>15</sup> Glyco-engineering could be achieved by several methods. A common approach is through genetic modification of specific glycosyltransferases or glycosidases in the glycosylation pathway of host cells. Another approach is to modulate the culture condition, such as culture media enriched with glycosylation precursors or inhibitors, or to manipulate culture parameters such as dissolved oxygen, temperature, pH, osmolality, and culture type.<sup>16</sup> All of these approaches are able to alter the N-

glycosylation profile, but none of them could produce a homogeneous glycoform with a single type of glycosylation for use in the study of the effect of glycan on protein folding and function. Recently, the most practical way to acquire homogeneous glycoprotein is by glycan remodeling *in vitro* using endoglycosidases and glycosyltransferases.<sup>17,18</sup> In this process, a combination of endoS and fucosidase was used to obtain antibodies containing a mono-GlcNAc residue at N297, which was further extended with specific glycans to obtain IgGs with a homogeneous, well-defined glycan for functional study. It was found that a glycoform with a human sialo-complex type (hSCT) glycan of biantennary N-glycan structure without core-fucosylation but with two terminal α2,6-linked sialic acids is an optimized N-glycan for the enhancement of ADCC, CDC, and anti-inflammatory activities.<sup>19</sup> The glycoform increases the binding affinity of IgG<sub>hSCT</sub> to FcγRIIA, FcγRIIB, and especially FcγRIIIA, by more than 9-fold and retains similar affinity to C1q protein. The enhanced affinity to Fc receptors provided better effector functions. In addition, the glyco-engineered anticancer IgGs showed better EC<sub>50</sub> activity for cancer clearance by 10-fold, and an antiviral IgG<sub>hSCT</sub> provided significantly improved protection in an infected mouse model. Thus, the 2,6-hSCT instead of 2,3-hSCT glycosylation is a

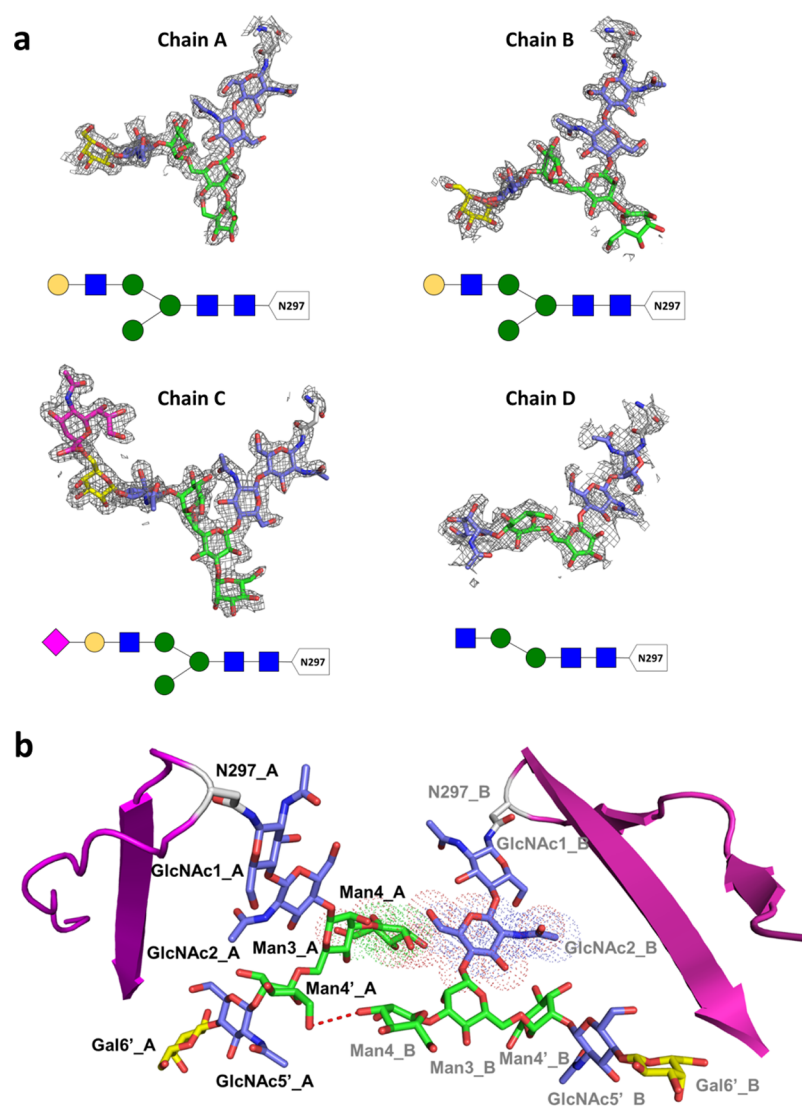


**Figure 2.** Glycan structures in electron density map of  $Fc_{hSCT}$ . (a)  $2F_o - F_c$  electron density map (contoured at  $1.2\sigma$ ) of glycans in  $Fc_{hSCT}$  structure. Ordered glycan residues are shown schematically below using symbol nomenclature according to Consortium for Functional Glycomics. (b) Glycan-glycan interaction networks in compact  $Fc_{hSCT}$ . Hydrogen bond is shown as red dashed line; van der Waals interaction of carbohydrates is shown as dotted sphere surrounding interacting residues.

common and optimized structure for the effector function enhancement of therapeutic antibodies.<sup>19</sup>

Although many Fc domain structures were solved at high resolution, none of them was determined to show the structure of Fc with homogeneous glycoform with enhanced ADCC, CDC, and anti-inflammatory activities. Here, we reported the first crystal structure of such glyco-engineered Fc ( $Fc_{hSCT}$ ), and explained the relationship between conformation plasticity and effector functions.

## RESULTS AND DISCUSSION

**Structure of Two Forms of  $Fc_{hSCT}$ .** A structure of  $Fc_{hSCT}$  with 1.85 Å resolution was determined in space group  $P2_1$  with two Fc dimers in each asymmetric unit (a.s.u.). Models were built from residues 236–444 of A, B, and C chains. The D chain contains residues 240–444, with missing residues in the loops at 266–270, 294–296, and 325–328 (Figure 1a). Both  $Fc_{hSCT}$  dimers have a classical immunoglobulin fold. The  $C_H2$  domains in the Fc dimer do not contact with each other directly but have some interaction mediated by the N297-

linked glycans (see below). On the other hand, the  $C_H3$  domains tightly pack with each other to form the foundation for dimer association. There is no direct interaction between the two  $Fc_{hSCT}$  dimers in single a.s.u.

The two dimers in the asymmetric unit exhibit different orientation of  $C_H2$  domains. The A and B chains form a relatively “compact” conformation, whereas the C and D chains exhibit a more “open” conformation, defined by the separation of the two  $C_H2$  domains while the two  $C_H3$  domains were well-aligned (Figure 1b). A root-mean-square deviation (RMSD) value between these two forms of dimer is 1.40 Å (calculated for the 402 paired  $C\alpha$  atoms). The RMSD value of aligned  $C_H3$  domains is 0.24 Å, while that of superimposed  $C_H2$  domains is 2.6 Å, suggesting that the conformational difference is mainly caused by the orientation of  $C_H2$  rather than  $C_H3$ . In order to clearly show the separation of two  $C_H2$  domains, a set of measurements including the distances between the paired  $C\alpha$  atoms (F241, N297, R301, and P329) on each  $C_H2$  domain was used.<sup>20</sup> The four distance indices of the compact dimer (A, B chains) are 19.2, 27.2, 27.2, and 21.5 Å, while the indices of

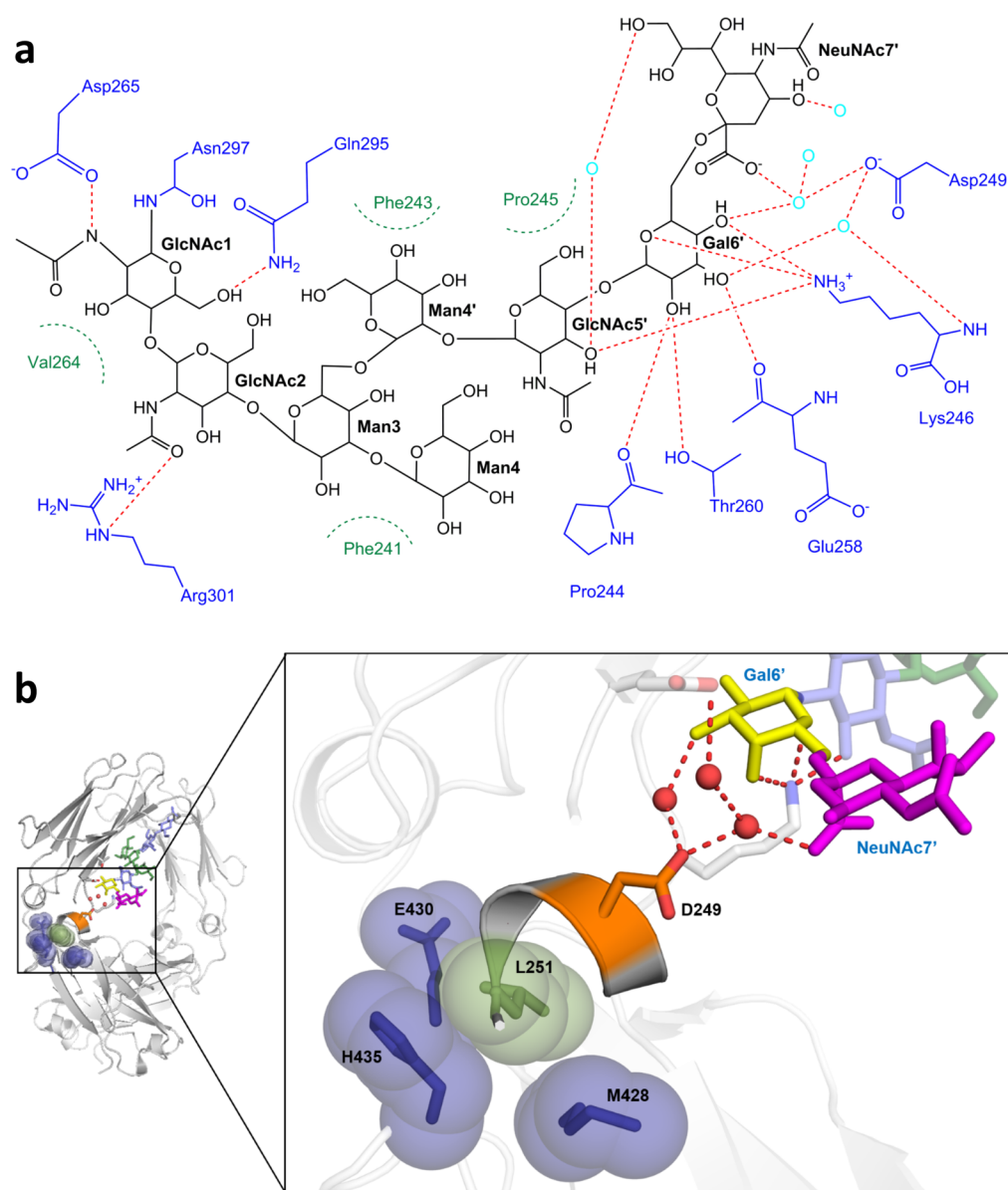


**Figure 3.** Protein–glycan interaction networks in  $Fc_{hSCT}$ . (a) Interactions between hSCT glycan and Fc protein. The glycans are shown in black and proteins in blue. Water oxygens are colored in cyan. Hydrogen bonds are defined with distance  $\leq 3.3 \text{ \AA}$  between selected atoms and shown in red dashed lines. Hydrophobic interactions are shown as eyelash symbols in green. (b) Interactions near the terminal sialic acid residue and pivot region between  $C_{H2}$  and  $C_{H3}$  domains. Hydrogen bonds are shown as red dashed lines; hydrophobic packing is shown as sphere.

open dimer (C, D chains) are 22.2, 31.4, 32.4, and 26.6  $\text{\AA}$ , further supporting the idea that the two dimers have a near 4  $\text{\AA}$  difference in openness of their  $C_{H2}$  domains.

**Structure Comparison of  $Fc_{hSCT}$  with Other Fc Glycoforms.** The  $Fc_{hSCT}$  structures were compared with the solved Fc structure with diverse glycosylation forms or mutations by superimposing their  $C_{H3}$  domains. The glycoforms, including heterogeneous type (3DO3), G2F ( $\text{Gal}_2\text{GlcNAc}_2\text{Man}_3\text{GlcNAc}_2\text{Fuc}$ ) type (4KU1), high mannose ( $\text{Man}_9\text{GlcNAc}_2$ ) type (2WAH), and deglycosylated type (3DNK), are listed according to the decreasing lengths of glycan chains. One structure of Fc with the GASDALIE mutation (5D4Q) reported to enhance its ADCC was also included in the comparison. The compact form of  $Fc_{hSCT}$  shows the narrowest separation of  $C_{H2}$  domains than any other reported Fc structures (Figure 1c). With a comparison of the RMSD values of different Fc glycoforms, we found that the

G2F type is most similar to the compact form (RMSD = 0.89  $\text{\AA}$ ) but different from the open form (RMSD = 1.41  $\text{\AA}$ ), while the high mannose type Fc is more like the open form (RMSD = 0.87  $\text{\AA}$ ) but different from the compact form (RMSD = 2.23  $\text{\AA}$ ). Surprisingly, the separations of the  $C_{H2}$  domains of two Fcs, the deglycosylated type Fc, which are believed to lose the binding affinity to Fc receptor,<sup>21,22</sup> and the GASDALIE mutant, which has been suggested to enhance the FcR binding,<sup>23</sup> are located in between the compact form and open form. This result suggested that the openness of the  $C_{H2}$  domains may not directly correlate with glycan status or Fc receptor binding affinity.

Two forms of  $Fc_{hSCT}$  were also aligned with other solved Fc structures in complex with Fc $\gamma$ RIIIA (Figure 1d), which are similar to the open form of  $Fc_{hSCT}$ , with the RMSD value in the range of 0.708–1.568  $\text{\AA}$ , and different from the compact form of  $Fc_{hSCT}$ , with the RMSD value in the range of 1.486–2.771  $\text{\AA}$ .

The compact form is not possible to accept the Fc $\gamma$ R1IIIA binding due to the narrow space between two C<sub>H</sub>2 domains. The open form of Fc<sub>hSCT</sub> is similar to the Fc structures in complex with Fc $\gamma$ R1IIIA. However, the open form with enough space between C<sub>H</sub>2 domains does not guarantee good ADCC activity, since one Fc glycoform with core-fucosylation also possesses open conformation, but it is known to have low ADCC activity.<sup>24</sup>

Currently, there are only two available Fc structures with enzymatically modified homogeneous glycan. One is provided here with the hSCT glycan, and the other is an anti-inflammatory IgG carrying the G2S2F type glycan (PDB entry: 4Q6Y).<sup>14,25</sup> When the glycan type is compared between these two structures, the G2S2F form is similar to the hSCT form, with biantennary penta-saccharide and additions of galactose, terminal sialic acid, and the core fucose (named as di-sFc). Recent studies suggested that antibodies with core-fucosylation show a large decrease in Fc $\gamma$ R1IIIA binding and lead to a weaker ADCC.<sup>11,12,24,26,27</sup> Thus, IgG<sub>hSCT</sub> shows optimized ADCC while the G2S2F type IgG has an anti-inflammatory property. Interestingly, the di-sFc structure also contains two Fc dimers in one a.s.u. and shows an open and a closed conformation, and they are different by the separation of C<sub>H</sub>2 domains, similar to our Fc<sub>hSCT</sub> result. Alignment of our two forms of Fc<sub>hSCT</sub> structures with theirs showed that both the open forms are similar to each other (RMSD = 0.457 Å), but the compact form of Fc<sub>hSCT</sub> and closed form of di-sFc are different (RMSD = 1.906 Å; Figure 1e). The separations of C<sub>H</sub>2 domains in the compact form of Fc<sub>hSCT</sub> and the closed form of di-sFc are similar, but they orient in different directions. Thus, the structures of Fc<sub>hSCT</sub> and di-sFc may provide at least three structural snapshots of the various states of Fc with disialylation.

**Glycan Latches in Fc<sub>hSCT</sub> Dimer.** In the Fc<sub>hSCT</sub> structure, the electron density of the biantennary N-linked glycans of four chains was clearly visible (Figure 2a). In agreement with a previous NMR study, the 1,3-arm of glycan chains is relatively more flexible than the 1,6-arm<sup>28</sup> and could only be seen at the first branched mannose residue in our structure of A, B, and C chains. The 1,6-arm of A and B chains could be seen with a terminal galactose residue, while in the C chain, the terminal sialic acid residue could be clearly seen. Due to the flexible nature of loops in the D chain, the electron density was missing for residues 266–270, 294–296, and 325–328, and only a glycan with five residues was observed.

In the compact form of Fc<sub>hSCT</sub>, the hSCT glycans of A–B chains make contact with each other by two interactions. The equatorial OH group at the C-3 position of Man4 (B chain) plays a role as hydrogen bond donor for the O6 of Man4' at the 1,6-arm (A chain). In addition, Man4 at the 1,3-arm of the A chain has a van der Waals interaction with the core GlcNAc2 of B chain (Figure 2b). These interactions work together as two latches to pull the C<sub>H</sub>2 domains together. The C<sub>H</sub>2 domains in the Fc dimer do not make contact with each other in the protein, so the intermolecular glycan–glycan interactions are the main force for the narrow separation of C<sub>H</sub>2 in compact Fc<sub>hSCT</sub>.

**Terminal Sialic Acid Residue Interacts with the Pivot Region of Fc.** In the open form of Fc<sub>hSCT</sub>, the glycan structure of the C chain could be unambiguously positioned to the terminal sialic acid residue at the 1,6-arm (Figure 2a). The details of the intramolecular glycan–glycan or glycan–protein interaction are shown in Figure 3a. The sialic acid residue does

not directly make contact with any protein residues, but its interactions are mediated with several ordered waters. For example, two hydrogen bonds were formed at O4 and O9, with two fixed waters, which are stabilized by the O3 atom of GlcNAc5' and the side chain of T260, respectively. In addition, Gal6' and NeuNAc7' residues form a water-mediated network with the main chain of K246, E258, and T260, and the side chain of D249. Interestingly, the D249 residue begins a short  $\alpha$ -helix through L251 (Figure 3b), which is the key residue at the pivot region between the C<sub>H</sub>2 and C<sub>H</sub>3 domains. The side chain atoms of L251 at the end of the short helix in C<sub>H</sub>2 form hydrophobic interactions with M428, E430, and H435 in the F–G loop of the C<sub>H</sub>3 domain, suggesting a “ball-in-socket” joint model.<sup>20,29</sup> Thus, the hSCT glycan chain may modulate the orientation of the C<sub>H</sub>2–C<sub>H</sub>3 domains through the D249–L251 helix by Gal6' and NeuNAc7' residues.

The  $\alpha$ 2,6-linked NeuNAc7' was fitted unambiguously in the electron density of Fc<sub>hSCT</sub> (Figure 2a). It is impossible to model an  $\alpha$ 2,3-linkage in both the compact and the open conformations, because the OH group at the C-3 position of Gal6' faces the protein surface and interacts with the backbone oxygen of E258 (Figure 3a). There is no space for NeuNAc to be added at the C-3 position without altering either the current compact or open Fc<sub>hSCT</sub> structures. Thus, we believed that the Fc structure with 2,3-sialylation adopts different conformation from the 2,6-hSCT linked Fc. The structural difference between 2,6- and 2,3-hSCT linked Fcs may correlate with our previous observation that  $\alpha$ 2,6-sialylation has better ADCC activity than the  $\alpha$ 2,3 type, where its activity is similar to the CHO cell expressed IgG with heterogeneous glycans.<sup>19</sup>

**IgG<sub>hSCT</sub> Enhanced ADCC Activity.** Since the hSCT glycan have been shown to enhance the ADCC activity of anticancer and antiviral IgGs both *in vitro* and *in vivo*,<sup>19</sup> we tested three glyco-engineered IgGs that target the Ebola virus surface glycoprotein, GP, which was overexpressed on HEK293T cells. Three anti-GP antibodies, 13C6, 4G7 (belonging to the therapeutic antibody mixture ZMapp),<sup>30</sup> and KZ52,<sup>31</sup> were glyco-engineered to have the homogeneous hSCT glycan. The ADCC activities of native- and hSCT-IgGs were tested by a luciferase reporter assay (Figure 4). Once the surface antigen GP on the target cell was recognized by the antibody, the Fc-glycosite region of the antigen–antibody complex could further bind to Fc $\gamma$ R1IIIA on the effector cell and trigger the downstream signaling to express a luciferase gene, which would show a light signal after substrate addition. The luciferase signal is thus quantitatively correlated with the ADCC activity. The 13C6<sub>hSCT</sub> antibody showed better effector function than its native form with heterogeneous glycans, with an EC<sub>50</sub> shifted from 0.270  $\mu$ g/mL to 0.104  $\mu$ g/mL. Native 4G7 and KZ52 show binding avidity to Fc $\gamma$ R1IIIA with K<sub>D</sub> values of 96.4 and 77.0 nM, respectively, while the K<sub>D</sub> values of 4G7<sub>hSCT</sub> and KZ52<sub>hSCT</sub> to Fc $\gamma$ R1IIIA are 13.5 and 12.9 nM, respectively. Interestingly, native 4G7 and KZ52 did not have measurable ADCC activity in our assay even with the antibody concentration up to 40  $\mu$ g/mL. It is possible that these two antibodies have their therapeutic function by binding and neutralizing the Ebola virus instead of ADCC killing.<sup>31,32</sup> However, the hSCT forms of these two antibodies showed “gain-of-function” in our ADCC assay. The EC<sub>50</sub> values of 4G7<sub>hSCT</sub> and KZ52<sub>hSCT</sub> were 0.219  $\mu$ g/mL and 0.387  $\mu$ g/mL, respectively. Mutations on Fc have been reported to make a nonactive antibody to gain ADCC activity.<sup>23,33</sup> This is the first case that the glycan modification not only enhances the binding

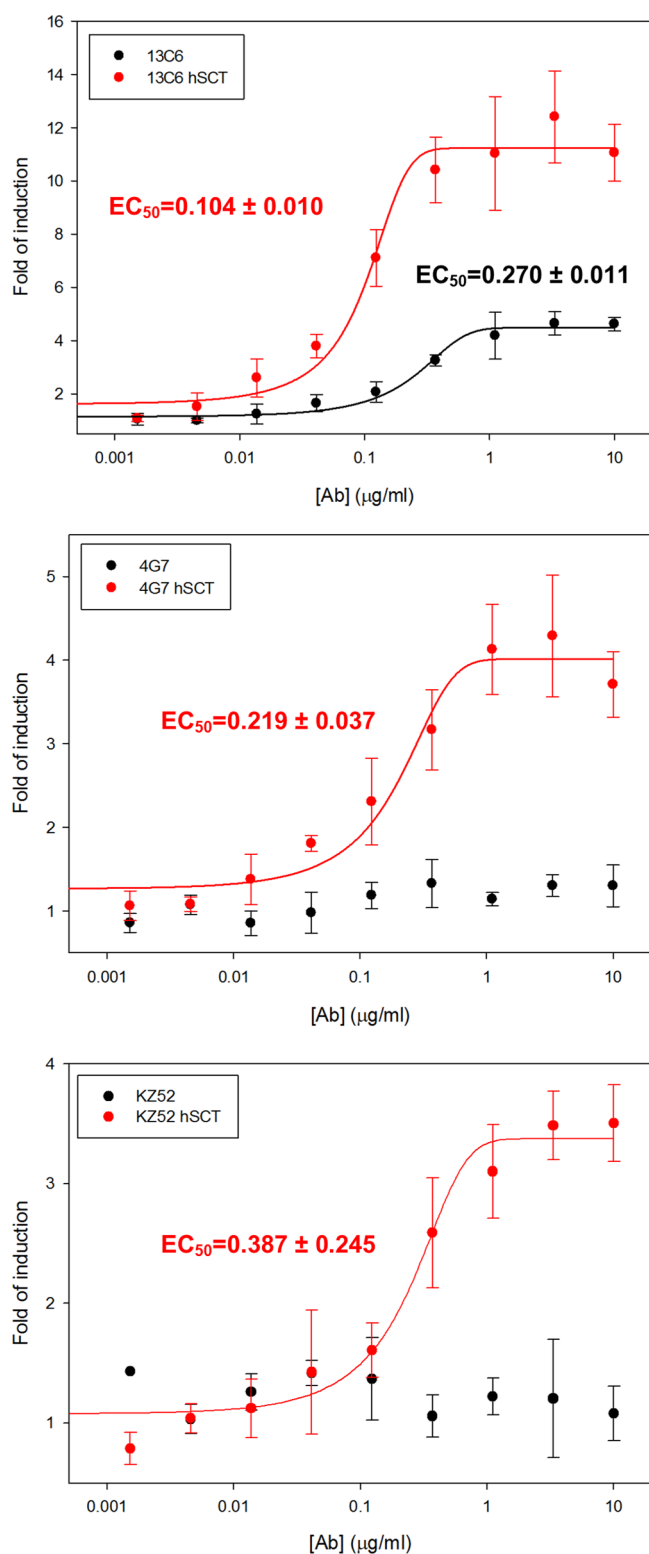


**Figure 4.** Antibody dependent cellular cytotoxicity assay of native IgG and IgG<sub>hSCT</sub>. The ADCC activity is shown as a fold of induction from a luciferase reporter assay. Curve fitting is conducted with a three-parameter sigmoid model to get the EC<sub>50</sub> value.

avidity of IgG to Fc receptors but also gives the antibody new activities.

**hSCT Modification Enhances the Fc Receptor Binding Avidity of Antigen–IgG Complex.** The immune complex formation is a sequential process. The antigen is first recognized

by the antibody Fab, and the Fc then further binds to the Fc receptors on the effector cell surface to activate the immune cell and trigger the downstream signaling and killing. Although the enhanced Fc receptor binding of IgG<sub>hSCT</sub> versus native IgG has been reported,<sup>19</sup> the avidity between FcγRIIIA and antigen-preoccupied IgG<sub>hSCT</sub> has not been studied. Here, we use biolayer interferometry (BLI) to study the binding kinetics with or without the presence of antigen (Figure 5). An anti-HER2 antibody, Trastuzumab, was first immobilized on the BLI sensor, and then soluble HER2 protein was added with 120 s of incubation. Interactions were measured by association with different concentrations of FcγRIIIA and dissociation in the buffer. The  $K_D$  value between FcγRIIIA and native Trastuzumab was 24.0 nM. However, with HER2 preoccupied on the Fab of Trastuzumab, the avidity had a 7-fold decrease to 169 nM. The lower affinity was due to the decrease of  $k_{on}$  and increase of  $k_{off}$  simultaneously. On the other hand, Trastuzumab<sub>hSCT</sub> had higher avidity to FcγRIIIA (9.9 nM) than the native form, as previously mentioned.<sup>19</sup> In the presence of antigen HER2, the avidity only slightly decreased (19.9 nM), with an increased off rate but the same on rate as the HER2-free condition. These data indicated that the antigen binding at Fab may affect the conformation of IgG, which in turn affects the FcγRIIIA binding. However, hSCT modification may modulate the Fc domain conformation to maintain similar binding avidity to the Fc receptor with or without the preoccupation of antigen. The enhancement of FcγRIIIA binding by hSCT glycan modification was only 2.4-fold in the absence of antigen, but an 8.5-fold avidity increase was observed in the presence of antigen. This result may partially explain why the anticancer antibodies with hSCT modification show nearly 10-fold better effector function in the *in vitro* ADCC assay, but only 2-fold enhancement in the FcγRIIIA binding assay because its measurements were performed in the absence of antigens.<sup>19</sup>

**hSCT Glycan Modulates the Conformational Plasticity of Fc.** hSCT modification shows two different effects on the conformation of Fc. First, the Fc structure is stabilized by two glycan latches to maintain the proper conformation of Fc but mediated by different glycan residues.<sup>34,35</sup> Our result suggested the role of N-glycosylation in maintaining the structure integrity of Fc and showed the possibility of diverse modes in glycan–glycan interactions. Second, the modulation by terminal sialic acid is observed at the pivot region through the D249–L251 helix. These two properties are semireciprocal: in the compact form, the two latches tightly link the C<sub>H</sub>2 domains, while the NeuNAc7' residue does not make contact with the D249 residue; in the open form, there is only one latch forming between the interchain Man4 residues, while NeuNAc7' interacts with D249 through a water-mediated manner, to push the L251 residue (ball) into the socket formed by M428, E430, and H435 residues (Figure 6).

Current structural information on disialylated Fc is limited, especially with regard to the differences between the 2,3- and 2,6-sialylations. Besides the hSCT glycoform reported here, the other two structures with terminal sialylation have core-fucosylation (PDB entries: 4Q6Y<sup>25</sup> and 4BYH<sup>36</sup>). These structures provided several snapshots, including at least a compact state and an open state conformation with disialylation. One NMR study of disialylated Fc suggested that the N-glycan chains occupy two distinct states: one with the 1,6-arm interacting tightly with the protein surface (as our observation in the crystal structures), the other with both

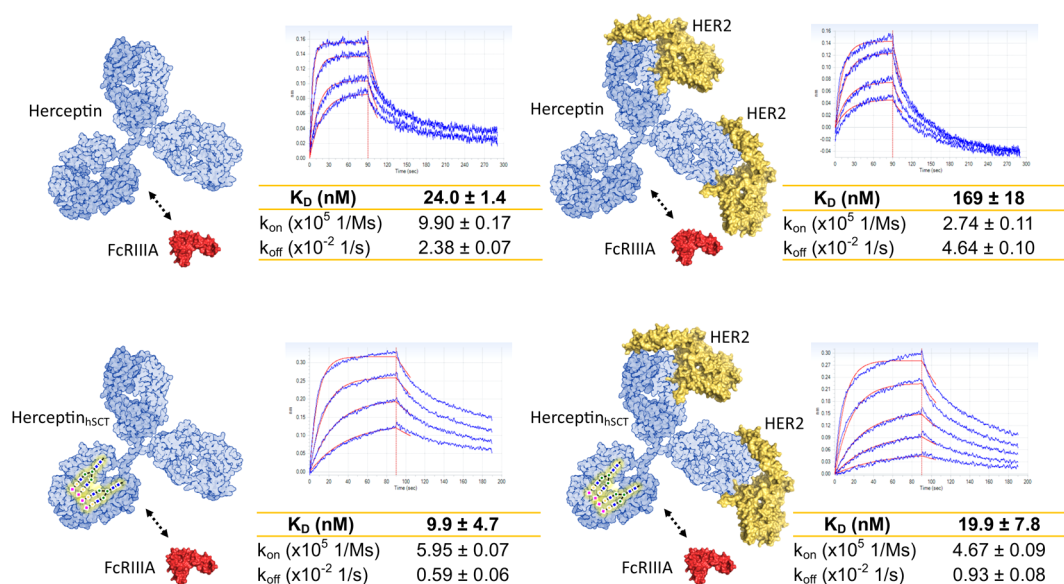


**Figure 5.** BLI analysis of a glyco-engineered antibody, with or without a bound antigen, binding to Fc $\gamma$ RIIIA. Sensorgrams of BLI are shown in blue with red fitting curves. Data analyses are performed using ForteBio Data Analysis Software with a 1:1 Langmuir binding model for  $k_{on}$ ,  $k_{off}$ , and  $K_D$  value determination.

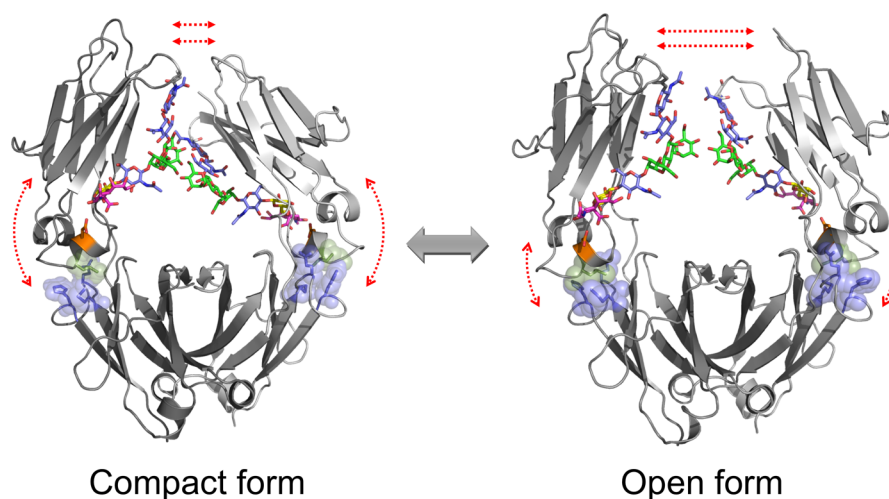


**Figure 6.** Modeled states of Fc<sub>hSCT</sub> structure. Glycan residues are modeled to terminal sialic acids according to reasonable carbohydrate geometry and colored as in Figure 2. D249 is shown as ball-and-stick, while L251, M428, E430, and H435 residues are shown as transparent spheres.

glycan terminals exposed to the bulk solvent and free from glycan–protein interactions.<sup>37</sup> The result suggests that the sialic acid addition may not simply determine the separation of C<sub>H</sub>2 domains but increase the conformational plasticity of Fc, which should be critical for effector functions. Although some studies suggested that the binding to Fc $\gamma$ RIIIA is not modulated by Fc sialylation,<sup>7</sup> recent studies, however, revealed that sialylation with 2,6-linkage instead of 2,3-linkage was responsible for the enhancement of ADCC,<sup>19</sup> pointing to a current problem of antibody production in CHO cells where the sialic acids are mainly in the 2,3-linkage. In addition, the study of Fc mutations together with core-fucosylation and disialylation<sup>38</sup> suggested that core-fucosylation plays a dominant role to inhibit the Fc $\gamma$ RIIIA binding, thus probably hindering the effect of  $\alpha$ 2,6-sialylation.

Either half or both faces of the terminal sialic acid residue are solvent-exposed. But we could not rule out the possibility that the sialic acid participates in some glycan–protein interaction,

such as the neonatal Fc receptor which binds to the interface of the C<sub>H</sub>2–C<sub>H</sub>3 domains, and is responsible for the long serum half-life of antibodies.<sup>39</sup>

Although static snapshots of crystal structures do not necessarily represent the flexibility of Fc protein in solution, out of over 40 unique crystal structures of Fc currently available with different glycoforms or in different crystal packings, only Fc with sialylation showed two conformations in a single crystal. The diverse conformations of Fc structures reported were disialylated and fucosylated.<sup>25</sup> Therefore, we suggest that the dual conformations observed in the current study are a hint of the intrinsic, structural flexibility of sialylated Fc. We suggest that the open conformation is likely the preferred conformation for binding with Fc $\gamma$ RIIIA to trigger immune functions, while the compact form with a larger C<sub>H</sub>2–C<sub>H</sub>3 interface may prefer to bind to the neonatal Fc receptor to extend the half-life of IgG.

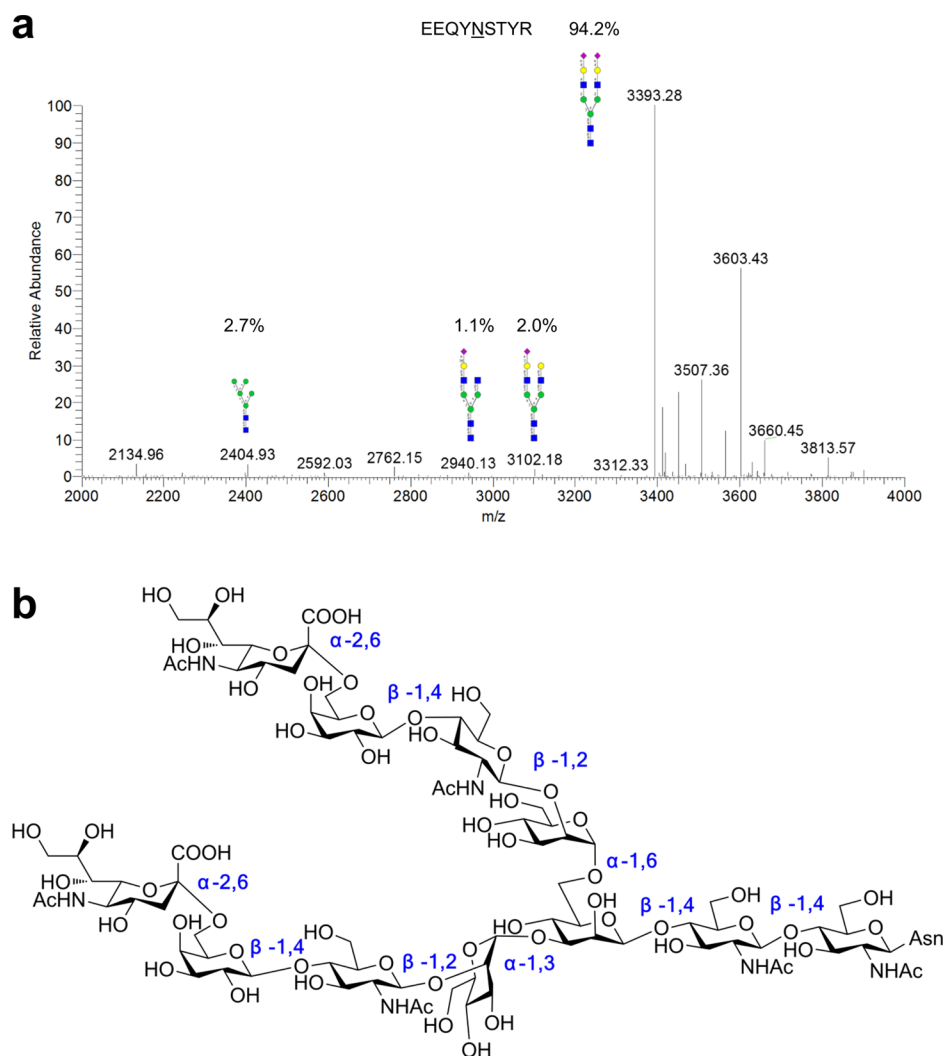


**Figure 7.** MS analysis of glycopeptide from IgG<sub>hSCT</sub>. (a) Representative Xtract LTQ Orbitrap XL MS spectra of trypsinized glycopeptides. (b) Schematic diagram of N297-linked hSCT glycan.

Sialylation also affects the IgG sensitivity to proteases. Sialylated Fc is more sensitive to papain than the asialylated Fc.<sup>35</sup> It has been speculated that the limited space between the two C<sub>H</sub>2 domains is just enough for the galactose residue. The bulkier sialic acid residue makes the Fc bulge and, hence, more accessible to proteases.<sup>40</sup> However, based on the current disialylated Fc structures,<sup>25,36</sup> the open form has a similar openness to other asialylated Fc structures, while the compact form shows more narrow space between the two C<sub>H</sub>2 domains. Thus, the negative charge of sialic acid or the conformational plasticity of sialylated Fc rather than the broader space may be the reason for sensitivity to proteolysis.

By enzymatically removing the glycan on Fc, it was shown that the avidity with FcγRs decreased as a result from increased conformational flexibility and a “closed” Fc structure.<sup>34</sup> However, the openness and structural stability may not simply correlate with good effector functions. For example, a Q295F/Y296A mutation of Fc was intended to increase the structural stability to enhance the effector functions. Nevertheless, the mutant with higher chemical and thermal stability unexpectedly shows a 100-fold decrease or total vanishing of Fc receptor binding.<sup>41</sup> Thus, greater flexibility of glycan chains rather than mutation in the Fc domain may contribute to the proper

conformational plasticity of Fc to modulate the effector functions.

In this work, we reported the first crystal structure of Fc<sub>hSCT</sub> with enhanced effector activities and proposed the relationship between conformation plasticity and effector functions. This work provided the structural basis for further glyco-engineering or IgG optimization in therapeutic applications. In addition, this is the first report that the hSCT modification not only enhances the ADCC activity but also gives antibodies with new functions. Last but not least, N-glycosylation may modulate the effector function of IgG cooperatively with an antigen. In our antigen-preoccupied binding experiment, the presence of antigen indeed affects the subsequent FcγRIIIA binding. Antibody prebound with FcγRIIIA also affects the avidity to its antigen (data not shown). Thus, further structural investigation of the ternary complex composed of antigen/antibody/Fc receptors will be critical for the understanding of the detailed mechanism of immune complex activation.

## METHODS

**Preparation of Homogeneous Glycoform Fc.** IgG with human 2,6-sialo-complex type glycan modification (IgG<sub>hSCT</sub>) was generated as previously mentioned.<sup>19</sup> IgG<sub>hSCT</sub> was further digested by papain-beads (Thermo Fisher Scientific) in 20 mM sodium phosphate, pH 7.0, with

10 mM EDTA and 20 mM cysteine for 6 h. Fab and Fc were separated by anion exchange Q column. The eluted Fc<sub>hSCT</sub> was subjected to size-exclusion Superdex 200 10/300 column (GE Healthcare Life Sciences) equilibrated with 20 mM Tris, pH 8.0, and 150 mM NaCl. Fractions corresponding to the Fc<sub>hSCT</sub> were pooled and concentrated to 21 mg mL<sup>-1</sup> using Amicon Ultra Centrifugal Filter Units (Millipore) with a molecular weight cutoff of 10 kDa. The purity of isolated Fc<sub>hSCT</sub> was examined by SDS-PAGE employing Coomassie staining for visualization. Trypsinized glycopeptide with a sequence of EEQYNSTYR showed a 94.2% homogeneous glycoform of hSCT in nanospray LC/MS (Figure 7a). Both the intact molecular weight and trypsin-digested segments indicated that there were no other modifications on IgG<sub>hSCT</sub>. In addition, O-glycosylation has been examined by mass spectroscopy. There was no O-glycosylation before and after glyco-engineering of trastuzumab, which was used in this study.

**Crystallization and Data Collection.** The initial crystallization screening was carried out using the mosquito Crystal crystallization robot (TTP Labtech) with commercial kits (Hampton Research). Crystals were obtained in a solution of 0.1 M sodium acetate trihydrate, pH 4.5, and 25% (w/v) PEG 3350. After optimization, the best single crystals were obtained by 1:1.5 mixing of the 21 mg mL<sup>-1</sup> Fc<sub>hSCT</sub> protein with 0.1 M sodium acetate trihydrate, pH 4.5, and 30% (w/v) PEG 3350 using a hanging-drop vapor-diffusion method at 20 °C. Diffraction-quality crystals of Fc<sub>hSCT</sub> were harvested, soaked in crystallization solution supplemented with 20% (v/v) ethylene glycol and flash-frozen in liquid nitrogen. Data collection was carried out at beamline BL41XU, SPring-8, Japan, using a wavelength of 1.000 Å and a temperature of 100 K. Diffraction images were processed and scaled with HKL2000 software (HKL Research).<sup>42</sup>

The crystals belong to the space group P2<sub>1</sub> with 1.85 Å resolution. A statistic table of data collection is shown as Table S1. The value of Matthew's coefficient is 2.55 Å<sup>3</sup>/Da for two Fc<sub>hSCT</sub> dimers in one a.s.u., corresponding to a solvent content of 51.76%.

**Structural Determination.** The structure of Fc<sub>hSCT</sub> was solved by molecular replacement with Phaser<sup>43</sup> in the Phenix package<sup>44</sup> using the structure of human IgG1 Fc (PDB entry: 3DO3) as the search model. In the initial solution, three C<sub>H2</sub> domains in one a.s.u. with poor electron-density fitting were deleted. One C<sub>H2</sub> domain and four C<sub>H3</sub> domains with correct positions were kept as a fixed model for second round molecular replacement using the C<sub>H2</sub> fragment of Fc as a search model. Carbohydrate molecules were added manually using a 2F<sub>o</sub> - F<sub>c</sub> electron density map contoured at 1.2σ. Further refinements were carried out using Coot<sup>45</sup> and Phenix. Glycan structure and geometry were checked with the PDB CARbohydrate RESidue check (PDBCARE)<sup>46</sup> and CARbohydrate Ramachandran Plot (CARP).<sup>47</sup> A statistic table of model building and refinement are shown in Supporting Information Table 1. All structural figures were generated with Pymol 1.3<sup>48</sup> and ChemDraw 15.0.

**Antibody Dependent Cellular Cytotoxicity (ADCC) Assay.** The ADCC activity assay was performed with a luciferase reporter bioassay kit (Promega). The HEK293T cells were maintained in DMEM medium (Gibco) supplemented with 10% (v/v) heat-inactivated fetal bovine serum and 1% (v/v) antibiotic-antimycotic solution (Gibco) and were transfected with Ebola-GP plasmid using a PolyJet transfection reagent (SignaGen) for 36 h before the assay. The transfected target cells were harvested and plated in 96-well microplates (5000 cells/well). Serial dilutions of native or glyco-engineered anti-Ebola-GP antibodies were added, followed by incubation with the NFAT engineered Jurkat cells (30 000 cells/well) expressing FcγRIIIA with the V158 variant for 5 h at 37 °C. The final effector to target cell ratio is 6:1. The readout was done through adding the Bio-Glow luciferase substrate and recorded by the Spectra Max M5 luminescence reader (Molecular Devices). The ADCC activity was calculated with the following formula: Fold of induction = (induced luminescence - background of buffer only)/(induction of no antibody control - background of buffer only). Data were fitted with a three-parameter sigmoid model to get the EC<sub>50</sub> value by SigmaPlot 12 software (Systat Software).

**Biolayer Interferometry (BLI) Analysis.** Expression and purification of FcγRIIIA followed the same protocol as previously

mentioned.<sup>19</sup> All the BLI experiments were performed on an Octet RED96 instrument (ForteBio) at 30 °C using TBST (20 mM Tris at pH 8.0, 150 mM NaCl, 0.005% (v/v) Tween 20) as a kinetic buffer.<sup>49</sup> Antihuman Fab-CH1 second Generation (FAB2G) biosensors were activated in advance. After 90 s of loading of native or glyco-engineered IgG antibody variants (25 μg/mL), the sensors were incubated in TBST or in the same buffer with 1 mM antigen, for normal kinetic or for antigen-preoccupied binding experiments, respectively. The binding kinetic measurement was performed with a baseline (120 s) in TBST, with various concentrations of FcγRIIIA (90 s) for association study, and the dissociation measurement was in TBST buffer (100 s). Data analysis and fitting were performed using ForteBio Data Analysis Software version 8.1 with a 1:1 Langmuir binding model for *k*<sub>on</sub>, *k*<sub>off</sub>, and *K*<sub>D</sub> value determination.

## ■ ASSOCIATED CONTENT

### 📄 Supporting Information

The Supporting Information is available free of charge on the ACS Publications website at DOI: 10.1021/acscchembio.7b00140.

Statistic table of data collection and refinement (PDF)

### Accession Codes

Atomic coordinates have been deposited to the Protein Data Bank with accession code 5GSQ.

## ■ AUTHOR INFORMATION

### Corresponding Authors

\*E-mail: [chwong@gate.sinica.edu.tw](mailto:chwong@gate.sinica.edu.tw).

\*E-mail: [cma@gate.sinica.edu.tw](mailto:cma@gate.sinica.edu.tw).

### ORCID

Chia-Lin Chen: 0000-0001-9490-6492

Chi-Huey Wong: 0000-0002-9961-7865

### Notes

The authors declare no competing financial interest.

## ■ ACKNOWLEDGMENTS

We thank D. Burton of the Scripps Research Institute for providing the antibody KZ52 expression vector; S.-C. Jao of the Biophysics Core Facility, Academia Sinica, for providing technical assistance for the biolayer interferometry experiment; J.-L. Lin and C.-H. Chen of the Genomics Research Center, Academia Sinica, for mass spectrometry analyses; W.-H. Lee, Academia Sinica, for discussion and critical reading of the manuscript; and K. Hasegawa, the staff of beamline 41XU, SPring-8, and the staff of TPS, NSRRRC, Taiwan, for assistance with crystallographic data collection. This work was supported by Academia Sinica and Ministry of Science and Technology, Taiwan (MOST 105-2325-B-001-007 to C.M.).

## ■ REFERENCES

- Reichert, J. M. (2012) Marketed therapeutic antibodies compendium. *MAbs* 4, 413–415.
- Vidarsson, G., Dekkers, G., and Rispen, T. (2014) IgG subclasses and allotypes: from structure to effector functions. *Front. Immunol.* 5, 520.
- Quast, I., and Lunemann, J. D. (2014) Fc glycan-modulated immunoglobulin G effector functions. *J. Clin. Immunol.* 34 (Suppl1), 51–55.
- Anthony, R. M., Wermeling, F., Karlsson, M. C., and Ravetch, J. V. (2008) Identification of a receptor required for the anti-inflammatory activity of IVIG. *Proc. Natl. Acad. Sci. U. S. A.* 105, 19571–19578.
- Sondermann, P., Pincetic, A., Maamary, J., Lammens, K., and Ravetch, J. V. (2013) General mechanism for modulating

immunoglobulin effector function. *Proc. Natl. Acad. Sci. U. S. A.* 110, 9868–9872.

(6) Yu, X., Vasiljevic, S., Mitchell, D. A., Crispin, M., and Scanlan, C. N. (2013) Dissecting the molecular mechanism of IVIg therapy: the interaction between serum IgG and DC-SIGN is independent of antibody glycoform or Fc domain. *J. Mol. Biol.* 425, 1253–1258.

(7) Le, N. P., Bowden, T. A., Struwe, W. B., and Crispin, M. (2016) Immune recruitment or suppression by glycan engineering of endogenous and therapeutic antibodies. *Biochim. Biophys. Acta, Gen. Subj.* 1860, 1655–1668.

(8) Collin, M., Shannon, O., and Bjorck, L. (2008) IgG glycan hydrolysis by a bacterial enzyme as a therapy against autoimmune conditions. *Proc. Natl. Acad. Sci. U. S. A.* 105, 4265–4270.

(9) Dalziel, M., Crispin, M., Scanlan, C. N., Zitzmann, N., and Dwek, R. A. (2014) Emerging principles for the therapeutic exploitation of glycosylation. *Science* 343, 1235681.

(10) Zou, G., Ochiai, H., Huang, W., Yang, Q., Li, C., and Wang, L. X. (2011) Chemoenzymatic synthesis and Fcγ receptor binding of homogeneous glycoforms of antibody Fc domain. Presence of a bisecting sugar moiety enhances the affinity of Fc to Fcγ<sub>3</sub> receptor. *J. Am. Chem. Soc.* 133, 18975–18991.

(11) Shields, R. L., Lai, J., Keck, R., O'Connell, L. Y., Hong, K., Meng, Y. G., Weikert, S. H., and Presta, L. G. (2002) Lack of fucose on human IgG1 N-linked oligosaccharide improves binding to human Fcγ<sub>3</sub> receptor and antibody-dependent cellular toxicity. *J. Biol. Chem.* 277, 26733–26740.

(12) Okazaki, A., Shoji-Hosaka, E., Nakamura, K., Wakitani, M., Uchida, K., Kakita, S., Tsumoto, K., Kumagai, I., and Shitara, K. (2004) Fucose depletion from human IgG1 oligosaccharide enhances binding enthalpy and association rate between IgG1 and Fcγ<sub>3</sub> receptor. *J. Mol. Biol.* 336, 1239–1249.

(13) Huhn, C., Selman, M. H., Ruhaak, L. R., Deelder, A. M., and Wuhrer, M. (2009) IgG glycosylation analysis. *Proteomics* 9, 882–913.

(14) Anthony, R. M., Nimmerjahn, F., Ashline, D. J., Reinhold, V. N., Paulson, J. C., and Ravetch, J. V. (2008) Recapitulation of IVIG anti-inflammatory activity with a recombinant IgG Fc. *Science* 320, 373–376.

(15) Liu, L. (2015) Antibody glycosylation and its impact on the pharmacokinetics and pharmacodynamics of monoclonal antibodies and Fc-fusion proteins. *J. Pharm. Sci.* 104, 1866–1884.

(16) Sha, S., Agarabi, C., Brorson, K., Lee, D. Y., and Yoon, S. (2016) N-Glycosylation Design and Control of Therapeutic Monoclonal Antibodies. *Trends Biotechnol.* 34, 835.

(17) Witte, K., Sears, P., Martin, R., and Wong, C. H. (1997) Enzymatic Glycoprotein Synthesis: Preparation of Ribonuclease Glycoforms via Enzymatic Glycopeptide Condensation and Glycosylation. *J. Am. Chem. Soc.* 119, 2114–2118.

(18) Huang, W., Giddens, J., Fan, S. Q., Toonstra, C., and Wang, L. X. (2012) Chemoenzymatic glycoengineering of intact IgG antibodies for gain of functions. *J. Am. Chem. Soc.* 134, 12308–12318.

(19) Lin, C. W., Tsai, M. H., Li, S. T., Tsai, T. I., Chu, K. C., Liu, Y. C., Lai, M. Y., Wu, C. Y., Tseng, Y. C., Shivatare, S. S., Wang, C. H., Chao, P., Wang, S. Y., Shih, H. W., Zeng, Y. F., You, T. H., Liao, J. Y., Tu, Y. C., Lin, Y. S., Chuang, H. Y., Chen, C. L., Tsai, C. S., Huang, C. C., Lin, N. H., Ma, C., Wu, C. Y., and Wong, C. H. (2015) A common glycan structure on immunoglobulin G for enhancement of effector functions. *Proc. Natl. Acad. Sci. U. S. A.* 112, 10611–10616.

(20) Teplyakov, A., Zhao, Y., Malia, T. J., Obmolova, G., and Gilliland, G. L. (2013) IgG2 Fc structure and the dynamic features of the IgG CH2-CH3 interface. *Mol. Immunol.* 56, 131–139.

(21) Jefferis, R., and Lund, J. (2002) Interaction sites on human IgG-Fc for Fcγ<sub>3</sub> receptor: current models. *Immunol. Lett.* 82, 57–65.

(22) Smith, P., DiLillo, D. J., Bournazos, S., Li, F., and Ravetch, J. V. (2012) Mouse model recapitulating human Fcγ<sub>3</sub> receptor structural and functional diversity. *Proc. Natl. Acad. Sci. U. S. A.* 109, 6181–6186.

(23) Ahmed, A. A., Keremane, S. R., Vielmetter, J., and Bjorkman, P. J. (2016) Structural characterization of GASDALIE Fc bound to the activating Fc receptor Fcγ<sub>3</sub> receptor. *J. Struct. Biol.* 194, 78–89.

(24) Ferrara, C., Grau, S., Jager, C., Sondermann, P., Brunker, P., Waldhauer, I., Hennig, M., Ruf, A., Rufer, A. C., Stihle, M., Umana, P., and Benz, J. (2011) Unique carbohydrate-carbohydrate interactions are required for high affinity binding between Fcγ<sub>3</sub> and antibodies lacking core fucose. *Proc. Natl. Acad. Sci. U. S. A.* 108, 12669–12674.

(25) Ahmed, A. A., Giddens, J., Pincetic, A., Lomino, J. V., Ravetch, J. V., Wang, L. X., and Bjorkman, P. J. (2014) Structural characterization of anti-inflammatory immunoglobulin G Fc proteins. *J. Mol. Biol.* 426, 3166–3179.

(26) Mizushima, T., Yagi, H., Takemoto, E., Shibata-Koyama, M., Isoda, Y., Iida, S., Masuda, K., Satoh, M., and Kato, K. (2011) Structural basis for improved efficacy of therapeutic antibodies on defucosylation of their Fc glycans. *Genes Cells* 16, 1071–1080.

(27) Nimmerjahn, F., and Ravetch, J. V. (2005) Divergent immunoglobulin g subclass activity through selective Fc receptor binding. *Science* 310, 1510–1512.

(28) Barb, A. W., and Prestegard, J. H. (2011) NMR analysis demonstrates immunoglobulin G N-glycans are accessible and dynamic. *Nat. Chem. Biol.* 7, 147–153.

(29) Hanson, Q. M., and Barb, A. W. (2015) A perspective on the structure and receptor binding properties of immunoglobulin G Fc. *Biochemistry* 54, 2931–2942.

(30) Qiu, X., Wong, G., Audet, J., Bello, A., Fernando, L., Alimonti, J. B., Fausther-Bovendo, H., Wei, H., Aviles, J., Hiatt, E., Johnson, A., Morton, J., Swope, K., Bohorov, O., Bohorova, N., Goodman, C., Kim, D., Pauly, M. H., Velasco, J., Pettitt, J., Olinger, G. G., Whaley, K., Xu, B., Strong, J. E., Zeitlin, L., and Kobinger, G. P. (2014) Reversion of advanced Ebola virus disease in nonhuman primates with ZMapp. *Nature* 514, 47–53.

(31) Lee, J. E., Fusco, M. L., Hessell, A. J., Oswald, W. B., Burton, D. R., and Saphire, E. O. (2008) Structure of the Ebola virus glycoprotein bound to an antibody from a human survivor. *Nature* 454, 177–182.

(32) Murin, C. D., Fusco, M. L., Bornholdt, Z. A., Qiu, X., Olinger, G. G., Zeitlin, L., Kobinger, G. P., Ward, A. B., and Saphire, E. O. (2014) Structures of protective antibodies reveal sites of vulnerability on Ebola virus. *Proc. Natl. Acad. Sci. U. S. A.* 111, 17182–17187.

(33) DiLillo, D. J., Tan, G. S., Palese, P., and Ravetch, J. V. (2014) Broadly neutralizing hemagglutinin stalk-specific antibodies require Fcγ<sub>3</sub> interactions for protection against influenza virus in vivo. *Nat. Med.* 20, 143–151.

(34) Krapp, S., Mimura, Y., Jefferis, R., Huber, R., and Sondermann, P. (2003) Structural Analysis of Human IgG-Fc Glycoforms Reveals a Correlation Between Glycosylation and Structural Integrity. *J. Mol. Biol.* 325, 979–989.

(35) Raju, T. S. (2008) Terminal sugars of Fc glycans influence antibody effector functions of IgGs. *Curr. Opin. Immunol.* 20, 471–478.

(36) Crispin, M., Yu, X., and Bowden, T. A. (2013) Crystal structure of sialylated IgG Fc: implications for the mechanism of intravenous immunoglobulin therapy. *Proc. Natl. Acad. Sci. U. S. A.* 110, E3544–3546.

(37) Barb, A. W., Meng, L., Gao, Z., Johnson, R. W., Moremen, K. W., and Prestegard, J. H. (2012) NMR characterization of immunoglobulin G Fc glycan motion on enzymatic sialylation. *Biochemistry* 51, 4618–4626.

(38) Yu, X., Baruah, K., Harvey, D. J., Vasiljevic, S., Alonzi, D. S., Song, B. D., Higgins, M. K., Bowden, T. A., Scanlan, C. N., and Crispin, M. (2013) Engineering hydrophobic protein-carbohydrate interactions to fine-tune monoclonal antibodies. *J. Am. Chem. Soc.* 135, 9723–9732.

(39) Ying, T., Ju, T. W., Wang, Y., Prabakaran, P., and Dimitrov, D. S. (2014) Interactions of IgG1 CH2 and CH3 Domains with FcRn. *Front. Immunol.* 5, 146.

(40) Raju, T. S., and Lang, S. E. (2014) Diversity in structure and functions of antibody sialylation in the Fc. *Curr. Opin. Biotechnol.* 30, 147–152.

(41) Chen, W., Kong, L., Connelly, S., Dendle, J. M., Liu, Y., Wilson, I. A., Powers, E. T., and Kelly, J. W. (2016) Stabilizing the CH2

Domain of an Antibody by Engineering in an Enhanced Aromatic Sequon. *ACS Chem. Biol.* 11, 1852.

(42) Otwinowski, Z., and Minor, W. (1997) Processing of X-ray diffraction data collected in oscillation mode. *Methods Enzymol.* 276, 307–326.

(43) McCoy, A. J., Grosse-Kunstleve, R. W., Adams, P. D., Winn, M. D., Storoni, L. C., and Read, R. J. (2007) Phaser crystallographic software. *J. Appl. Crystallogr.* 40, 658–674.

(44) Adams, P. D., Afonine, P. V., Bunkoczi, G., Chen, V. B., Davis, I. W., Echols, N., Headd, J. J., Hung, L. W., Kapral, G. J., Grosse-Kunstleve, R. W., McCoy, A. J., Moriarty, N. W., Oeffner, R., Read, R. J., Richardson, D. C., Richardson, J. S., Terwilliger, T. C., and Zwart, P. H. (2010) PHENIX: a comprehensive Python-based system for macromolecular structure solution. *Acta Crystallogr., Sect. D: Biol. Crystallogr.* 66, 213–221.

(45) Emsley, P., and Cowtan, K. (2004) Coot: model-building tools for molecular graphics. *Acta Crystallogr., Sect. D: Biol. Crystallogr.* 60, 2126–2132.

(46) Lutteke, T., and von der Lieth, C. W. (2004) pdb-care (PDB carbohydrate residue check): a program to support annotation of complex carbohydrate structures in PDB files. *BMC Bioinf.* 5, 69.

(47) Lutteke, T., Frank, M., and von der Lieth, C.-W. (2005) Carbohydrate Structure Suite (CSS): analysis of carbohydrate 3D structures derived from the PDB. *Nucleic Acids Res.* 33, D242–D246.

(48) *The PyMOL Molecular Graphics System*, version 1.8; Schrodinger, LLC: Cambridge, MA, 2015.

(49) Yu, Y., Mitchell, S., Lynaugh, H., Brown, M., Nobrega, R. P., Zhi, X., Sun, T., Caffry, I., Cao, Y., Yang, R., Burnina, I., Xu, Y., and Estep, P. (2016) Understanding ForteBio's Sensors for High-Throughput Kinetic and Epitope Screening for Purified Antibodies and Yeast Culture Supernatant. *J. Biomol. Screening* 21, 88–95.